



# Study on Single-Particle Crushing Strength-Size Effect of Recycled Aggregate

Qingdong Gao

Lanzhou Jiaotong University, Lanzhou 730070, China

E-mail: 1430484401@qq.com

**Abstract.** With the elevated production of municipal construction waste, the use of construction and demolition waste as recycled aggregate (RA) in the subgrade has become a sustainable and environmentally friendly disposal method. In order to reveal the single-particle crushing behavior of different recycled aggregates, particle scanning and single-particle crushing tests were carried out for recycled concrete aggregate (RCA) and recycled brick aggregate (RBA), which are the main components of recycled aggregates, to investigate their single-particle crushing modes, crushing strengths, and crushing energies, and the size effect of single-particle crushing strengths of recycled aggregates was analyzed by using the Weibull distribution function. The results show that: the single-particle crushing mode of recycled aggregate can be divided into single-peak, double-peak and multi-peak modes; recycled aggregate is mainly multi-peak crushing (64.17%); the larger the particle size of recycled aggregate particles is, the larger the peak force and crushing energy are, and the crushing stress decreases with the increase of the particle size; the peak force and crushing energy of RCA is significantly higher than that of RBA; and there is a size effect in both RCA and RBA; The crushing strength of single particles of RCA and RBA both satisfy the Weibull distribution better, and the Weibull modulus is 1.596 and 2.260 respectively, and the discrete shape of RCA is larger. The research results can provide theoretical basis for revealing the engineering construction of recycled aggregates.

**Keywords:** road engineering; recycled aggregate; single particle crushing; Weibull distribution

## 1 Introduction

With the rapid development of China's infrastructure, a large amount of construction and demolition waste has emerged, and the resource treatment of construction waste has become one of the problems that need to be solved for urban development [1]. If the construction waste can be processed and crushed as recycled aggregate for transportation construction, it can promote the green sustainable development and help the carbon peak and carbon neutral strategy [2]. Compared with natural aggregates, recycled aggregates are diverse materials with different shapes and particles are prone to breakage [3,4]. Therefore, the study of single-particle crushing behavior of recycled

aggregates and their strength characteristics can provide a theoretical basis for the utilization of recycled aggregates.

At present, many scholars have carried out single-particle crushing tests on gravel or pile stone bulk materials to investigate the effects of particle shape, particle size, material type and other factors on the crushing strength and crushing behavior of the particles. Wang et al. [5] showed that the Weibull distribution function of the distribution of the strength of the particles can be better described by the single-particle crushing test. Yin et al. [6] conducted single-particle crushing tests on calcareous soil particles and studied the relationship between the strength of calcareous soil particles and the crushing mode, and concluded that the crushing mode of calcareous soil is mainly explosive crushing. Wu et al. [7] classified the coral sand particle crushing into four modes: particle explosion, particle splitting, edge abrasion, and particle crushing. The particle size, particle morphology and initial microstructure all have effects on the particle crushing mode. Huang et al. [8] proposed a three-parameter Weibull distribution model and verified the size effect of particle crushing. Wang et al. [9] fitted the single-particle size and crushing intensity by power law index. These studies provide a theoretical basis for predicting the crushing behavior of particles of different sizes. Overall, current research has made important progress in the fields of crushing strength, crushing mode, and size effect of particles, and clarified the main factors affecting the crushing behavior of particles. [10] These research results not only deepen our understanding of the mechanical properties of bulk materials, but also provide strong theoretical support for the selection of materials and structural design in engineering practice. However, most of the current research still focuses on the particle crushing characteristics of traditional sand, gravel, pile stone and other materials, and there is still room for exploring the crushing characteristics and mechanical behaviors of such new special aggregates as construction and demolition waste from the perspective of individual particle crushing. At the same time, there are fewer studies that comprehensively consider the effect of particle size on the crushing characteristics of recycled aggregates from construction and demolition materials. In this paper, single-particle crushing tests were carried out on recycled aggregates with different particle sizes (including RBA and RCA) to comprehensively investigate the crushing modes, crushing strengths, and energy changes in the crushing process of single-particles of recycled aggregates.

## 2 Test Materials and Methods

The materials selected for this study were recycled aggregates obtained from construction and demolition crushing and screening, including RCA and RBA, as shown in Figure 1. The two different material types (RCA and RBA) selected were categorized into five particle size groups of 4.75-9.50 mm, 9.50-13.2 mm, 13.2-16 mm, 16.0-19.0 mm and 19.0-26.5 mm according to the particle size, and 60 particles in each particle size group, totaling 600 recycled aggregate particles were selected for the single-particle compression test. 3D scanner was used to scan the real shape of RA to extract the geometrical parameters of the minimum enclosing box of the particles as shown in Figure

1(d). The long (L), intermediate (I) and short (S) axes of the particles were obtained for calculating the equivalent particle size of the particles.

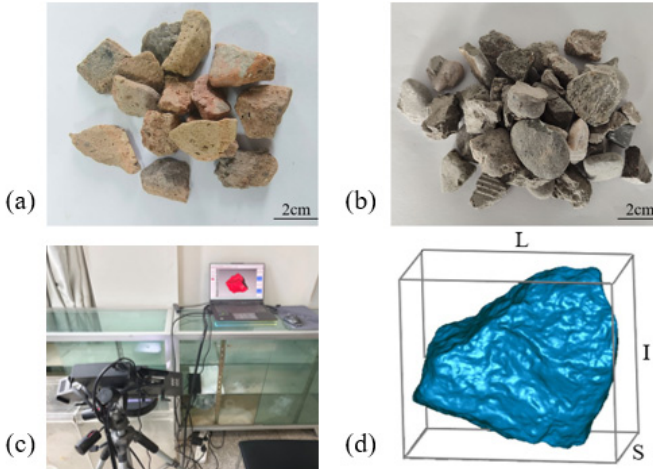


**Fig. 1.** Recycled aggregates and particle morphology acquisition (a)RBA;(b)RCA;(c) 3D scanner;(d) oriented bounding box.

The test apparatus for this test with single-particle compression test is a microcomputer-controlled electronic pressure testing machine, as shown in the Figure 2 The maximum range of the press is 300kN, the precision is 0.01kN, the loading speed can be adjusted between 0.01~50mm/min, and the loading speed of this test is 2mm/min. The whole test setup consists of three main parts: the loading system, the measurement and control system and the loading platform. The displacement control was used for uniform loading, and the load-displacement curve data were transmitted back to the computer in real time.

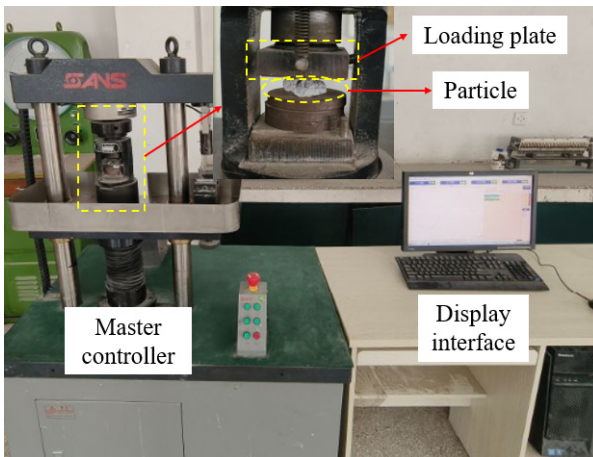


**Fig. 2.** Single-particle crushing compressor.

Before the test, the RA was placed on the bottom plate, adjusted to the specimen stability without deflection, and the displacement was used as the control condition, so that the upper loading plate just contacted the particles, and single-particle compression was carried out at a constant speed of 1mm/min, and the real-time recording of load-displacement curves was recorded in the course of the loading process, and the loading was stopped when the RA produced an obvious crack or the load-displacement curves decreased significantly. After unloading, the morphological characteristics of RA after crushing were observed and recorded, and the load-displacement curves were exported for data processing and analysis.

### 3 Experimental Results

#### 3.1 Single-Particle Crushing Modes

The single-particle crushing mode is generally divided into five types: surface grinding, single-pronged crushing, multi-pronged crushing, fracture, and crushing. However, in the actual particle compression process, there are generally multiple crushing modes at the same time [11]. Figure 3 shows the load-displacement relationship curve and the degree of fragmentation during the loading process of RCA single-particles. From the figure, it can be seen that at the initial loading, mainly for the particle adjustment stage, the RCA particles are more complete, with the increase of displacement, the load gradually increases; when the first peak point is reached, the RCA particles begin to crack, and the load-displacement curve begins to fluctuate; the loading displacement continues to increase, and the load-displacement curve shows a jagged shape with the polygonal breakage of the RCA particles; then there is a second peak point, and the cracks of the RCA particles are completely through; when the loaded displacement continues to increase, the load-displacement curve is completely through; and the RCA particle cracks are completely through. When the third peak point occurs, the RCA particles are completely cracked, and then can not continue to withstand the load, the test stops the load-displacement curve drops sharply, and the RCA particles are completely broken. The RBA particle crushing process is similar to that of the RCA particle crushing process.

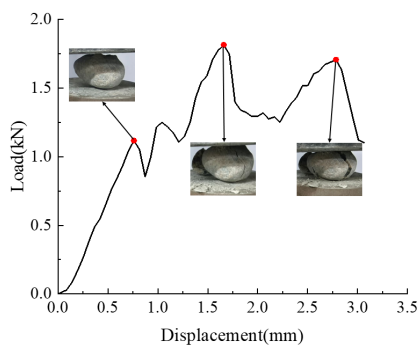


Fig. 3. Single-particle load-displacement curve and damage process.

Under the action of single-particle compression, the crushing mode of particles is mostly classified according to the crushing particle size and cracking mode. In this paper, we analyze the load-displacement curves obtained from single-particle compression tests, the number of fragments produced after particle crushing, and the particle characteristics, and classify the particle crushing mode into the following three types [12].

The first type is single peak. When the force is loaded to a certain point, the load-displacement curve decreases sharply, the RA particles break often with a crisp sound, and a particle breaks into two to three fragments with a neat fracture. The proportions of the single-peak crushing modes of RCA and RBA particles are 23.33% and 17.67%, respectively. The second type is double peak. This crushing mode load-displacement curve has two peak points, the load increases with the displacement, when the first peak point is reached, the RA will crack, the load-displacement curve will drop suddenly, as the test continues, the RA continues to withstand the load, and the particles are completely crushed after the emergence of the second peak point. The proportion of the double-peak crushing mode of the RCA and RBA particles are 15.67% and 61%, respectively. The third type is multi-peak. The load-displacement curve is sawtooth-like at the beginning of the test. There are many small peaks, at this time mainly for particle angular wear, as the test continues, cracks appear inside the particles, there will be multiple peak points, and finally the particles are broken into multiple fragments, and the test is over. The proportion of multi-peak crushing mode of RCA and RBA particles are 15% and 67.33%, respectively.

### 3.2 Single-Particle Crushing Strength

For the calculation of the crushing strength of single-particles, equation 1 is used and the equivalent particle size  $d$  is calculated using equation 2 [13].

$$\sigma = F / d^2 \quad (1)$$

$$d = \sqrt{\frac{I^2 + S^2}{2}} \quad (2)$$

Where  $\sigma$  is the compressive stress on the material,  $F$  is the magnitude of the load obtained in the test, and  $d$  is the equivalent particle size.

Figure 4 shows the load-displacement relationship curves and stress-strain relationship curves for different sizes of selected RBA particles. Where  $F_f$  is the maximum peak load and  $\sigma_f$  is the maximum peak stress. From Figure 4(a), it can be seen that the RBA particles exhibit a certain size effect, and the hair  $F_f$  of the particles increases as the particle size increases. When  $d = 4.75-9.5$  mm, the  $F_f$  is 0.27 kN, and when  $d = 19-26.5$  mm, the  $F_f$  is 2.41 kN, which is 815% larger than the former. However, the pattern in Figure 4(b) is opposite to that in Figure 4(a), where  $\sigma_f$  of RBA particles decreases with the increase of particle size. When  $d = 4.75-9.5$  mm,  $\sigma_f$  is 5.87 kN, and when  $d = 19-26.5$  mm,  $\sigma_f$  is 3.92 kN, which is 33.2% less than the former. For RCA particles, a similar size effect law exists. The reason for this is analyzed as, with the increase in the

particle size of RA particles, the internal pores and cracks of the particles increase, leading to a decrease in the strength of the particles.

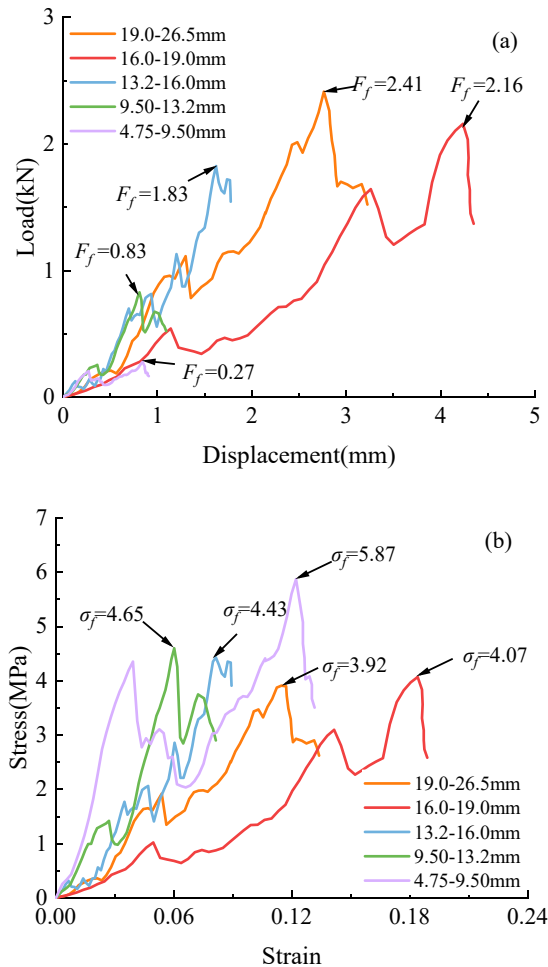


**Fig. 4.** Comparative strength curves for different particle sizes of RBA particles. (a) Load-displacement relationship curve; (b) Stress-strain relationship curve.

### 3.3 Single-Particle Crushing Energy

Single-particle crushing test can directly obtain the maximum peak load and displacement of single-particles when crushing occurs, after a simple conversion, you can get single-particle crushing strength. For single-particle crushing energy, can not be obtained directly through the test, but it has been shown that the single-particle crushing energy can be expressed as the integral function of the crushing load relative to the displacement [14], as shown in equation 3.

$$E_f = \int_0^{\Delta} F d\Delta \quad (3)$$

Where  $E_f$  is the single-particle crushing energy,  $F$  is the crushing load and  $\Delta$  is the displacement. The schematic diagram of single-particle crushing energy calculation is shown in Figure 5, where the shaded part is the single-particle crushing energy.

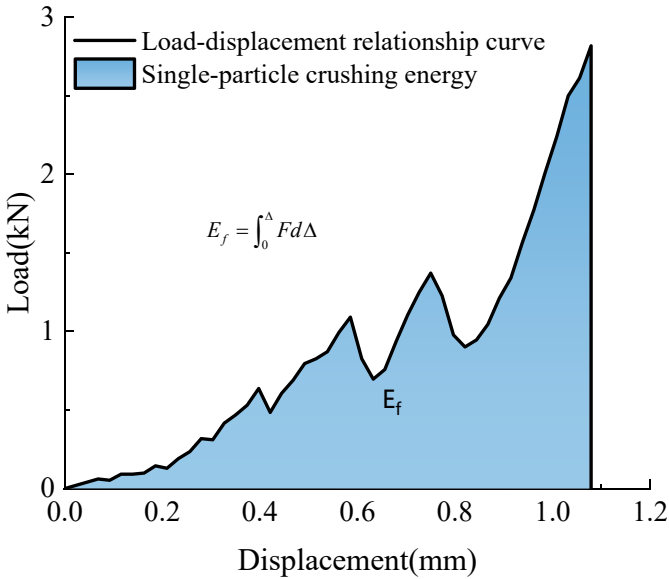


Fig. 5. Schematic diagram of single-particle crushing energy calculation.

Table 1. RCA and RBA single-particle crushing energy distribution.

particle size(mm)	Single-particle crushing energy (mJ)	
	RCA	RBA
4.75-9.5	172.04	114.14
9.5-13.2	315.15	251.32
13.2-16	717.27	310.25
16-19	893.38	402.13
19-26.5	1024.54	532.46

For the same particle size of the same material particles, their Single-particle crushing energy are not all the same, in order to ensure the reasonableness of the statistical analysis, this paper adopts the average Single-particle crushing energy under the same particle size instead of the Single-particle crushing energy  $E_f$  to be analyzed, as shown in Table 1. As can be seen from Table 1, the crushing energy of both RCA and RBA particles increases with the increase of particle size, which is due to the fact that the larger the particle size, the larger the energy contained, the larger the energy released when the particles undergo load to reach destruction. When  $d=4.75-9.5\text{mm}$ , the crushing energy of RCA and RBA particles are 172.04mJ and 114.14mJ respectively, and when  $d=19-26.5\text{mm}$ , the crushing energy of RCA and RBA particles are 1024.54mJ

and 532.46mJ, which are increased by 5.9 and 4.7 times respectively. The crushing energy of RCA particles at the same particle size were greater than the crushing energy of RBA particles, when  $d=4.75-9.5\text{mm}$ , the crushing energy of RCA particles was 1.5 times higher than that of RBA particles, and when  $d=19-26.5\text{mm}$ , the crushing energy of RCA particles was 1.9 times higher than that of RBA particles.

### 3.4 Weibull Distribution of Crushing Strength of Single-Particles

Unlike plastic materials, the breaking strength of brittle materials has large discrete characteristics. It has been shown that the Weibull distribution function is highly applicable to the strength of geotechnical granular materials[15,16], and its specific expression is shown in Equation 4.

$$P_s = \exp \left[ - \left( \frac{\sigma}{\sigma_{0,d}} \right)^m \right] \quad (4)$$

where  $P_s$  is the residual probability of particles, i.e., the ratio of the number of particles that did not break under a certain characteristic stress to the total number of particles, calculated by Equation 5.

$$P_s = \frac{n}{N} \quad (5)$$

Where  $n$  is the number of unbroken particles at that characteristic stress and  $N$  is the total number of particles tested, in this paper the total number of particles at a given particle size  $N=55$ .

In order to facilitate the use of Weibull distribution function to describe the distribution of single-particle crushing strength, so as to obtain the Weibull modulus  $m$ , and to identify the dispersion of single-particle crushing strength, the logarithmic transformation is performed on both sides of the equal sign of Equation 4, and the specific expression is shown in Equation 6.

$$\ln \left[ \ln \frac{1}{P_s} \right] = m (\ln \sigma - \ln \sigma_{0,d}) \quad (6)$$

$\sigma$  is a given certain characteristic stress, the characteristic strength  $\sigma_{0,d}$  of the particle is the characteristic stress corresponding to the residual probability of 37% (when  $\sigma = \sigma_{0,d}$ , the residual probability of  $P_s = 1/e \approx 37\%$ ), generally referred to as the 37% characteristic stress;  $m$  is the Weibull modulus, which characterizes the discrete nature of the particle strength, and the smaller the value of  $m$  is, the greater the discrete nature of the particle strength.

Figure 6 shows the residual probability curves of RCA and RBA particles with different particle sizes under a certain characteristic stress, and it can be found that RCA

and RBA show a similar change rule. That is, the particle size has a significant effect on the characteristic stress on RA, and the crushing strength of RA particles with smaller particle sizes is significantly higher than that of those with larger particle sizes. Among them, the characteristic stress of RCA particles is obviously larger than that of RCA particles. Under the same characteristic stress, the residual probability of the recycled granule particles with a particle size of 4.75-9.5 mm was significantly higher than that of the particles with a particle size of 19-26.5 mm. Corresponding to the above conclusion.

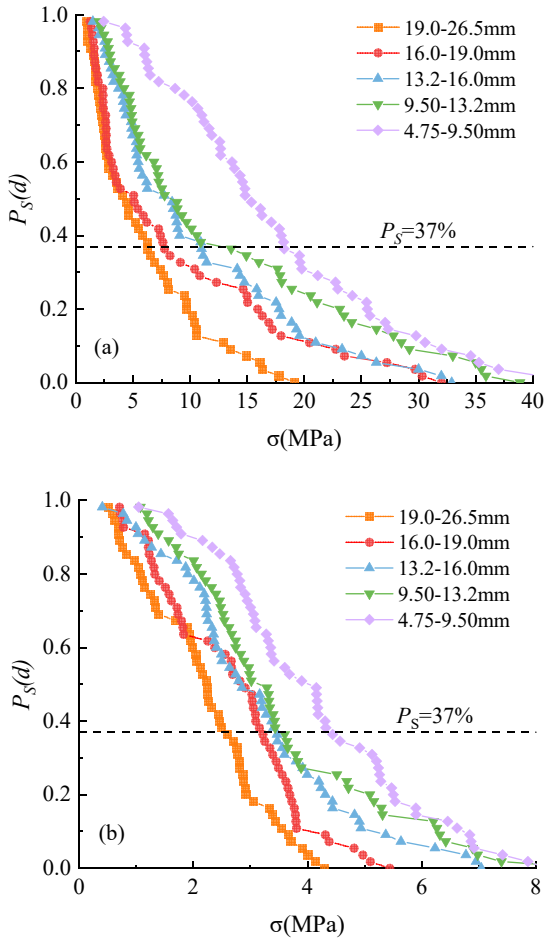


**Fig. 6.** Surviving probability of RA single-particles at different particle sizes. (a)RCA; (b)RBA.

From Figure 7, it can be seen that the strength of RA particles obeys the Weibull distribution model, and the difference in the value of Weibull modulus  $m$  for the same kind of RA is small, which is due to the fact that  $m$  itself represents the own property of the material. The calculated Weibull modulus and characteristic stresses of recycled

granules with different particle sizes are listed in Table 2. The average value of Weibull modulus  $m$  of five recycled granules with different particle sizes is taken as the Weibull modulus of the material, and the average Weibull modulus of concrete particles is 1.596, and that of brick particles is 2.260, which indicates that the concrete particles are more discrete is greater than brick particles.

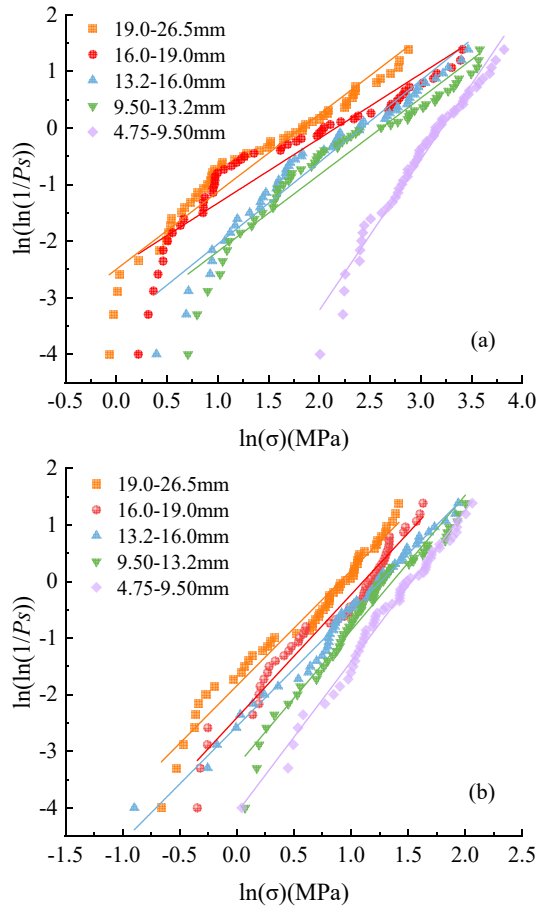


Fig. 7. Weibull distribution of RA particles. (a)RCA; (b)RBA.

Table 2. Weibull distribution and characteristic intensity of RA particles.

	$d$ (mm)	$d_0$ (mm)	$\sigma_{0,d}$ (MPa)	$m$	$\bar{m}$
RCA	4.75-9.5	6.11	18.233	2.517	1.596
	9.5-13.2	12.12	13.596	1.537	
	13.2-16	14.43	10.999	1.458	
	16-19	17.05	7.742	1.271	
	19-26.5	22.49	6.285	1.393	

RBA	4.75-9.5	6.98	4.401	2.509	2.260
	9.5-13.2	11.09	3.601	2.244	
	13.2-16	14.44	3.467	2.122	
	16-19	16.89	3.218	2.814	
	19-26.5	22.27	2.595	2.073	

### 3.5 Size Effects on the Crushing Strength of RA Particles

For the crushing strength of geotechnical granular materials, not only has the discrete nature, well have obvious size effect, regenerated aggregate is the same, according to the results of particle 3D scanning and reconstruction and the equivalent particle size  $d$ , the arithmetic average of the equivalent particle size of each file size particles as the average particle size of the file size of the average particle size  $d_0$ .

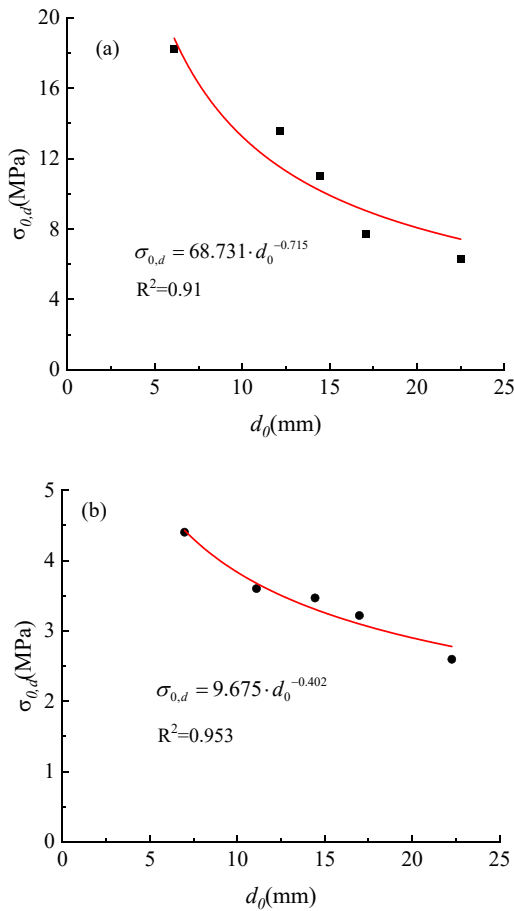


Fig. 8. The relationship between RA particle size and crushing strength. (a)RCA; (b)RBA.

Adopt the power function of each group of regenerated aggregates of crushing strength and the average particle size of particles to fit, then you can get the consideration of the The characteristic strength  $\sigma_{0,d}$  prediction formula for particle size. The correlation coefficients R2 of the relationship curves between the characteristic stresses of RCA and RBA and the average particle size are 0.91 and 0.953, respectively, as shown in Figure 8, and the characteristic stresses corresponding to each group of particle sizes of RBA are smaller than those of RCA, which is analyzed to be mainly due to the different composition of the material, and the brick has more pores and cracks inside the brick.

## 4 Conclusions

In this paper, 3D scanning was used to obtain the real morphology of recycled aggregates with five different particle sizes, and then single-particle crushing tests were carried out on the scanned recycled aggregate particles, and the results of RCA particles and RBA particles were comparatively analyzed to study the crushing mode, crushing strength, crushing energy, Weibull distribution and the size effect of crushing strength of recycled aggregate particles. The main conclusions are as follows:

Through the crushing process and load-displacement curve of recycled aggregate, the crushing mode of recycled aggregate is categorized into three types: single-peak, double-peak and multi-peak. Among them, multi-peak is the main crushing mode, accounting for 64.17%, while single-peak and double-peak account for 20.5% and 15.33%, respectively.

With the increase of particle size, the peak load of RCA and RBA particles gradually increases, while the corresponding peak stress decreases; its crushing energy also increases with the increase of particle size, and the peak load and crushing energy of RCA particles are larger than that of RBA particles under the same particle size.

The single-particle crushing strength of recycled aggregate particles conformed to the Weibull distribution, with average Weibull moduli of 1.596 and 2.260 for RCA and RBA, respectively, and a higher degree of dispersion for RCA. The single-particle characteristic stresses of recycled aggregates have obvious size effects. For the same type of particles, the characteristic stress decreases with the increase of particle size.

## References

1. ZHANG Jun-hui, DING (Le|Yue), ZHANG An-shun. Application of recycled aggregates from construction and demolition waste in subgrade engineering: a review[J]. China Journal of Highway and Transport, 2021, 34(10): 135-154.
2. KHAN Z A, BALUNAINI U, COSTA S, et al. A review on sustainable use of recycled construction and demolition waste aggregates in pavement base and subbase layers[J]. Cleaner Materials, 2024,13: 100266.
3. XU Y. In-situ shear strength of compacted demolition waste[J]. Powder Technology, 2019,352: 72-78.

4. ZHANG J, Le Ding, LI F, et al. Recycled aggregates from construction and demolition wastes as alternative filling materials for highway subgrades in China[J]. *Journal of Cleaner Production*, 2020,255: 120223.
5. JINWEI W, SHICHUN C, XIONGXIONG Z, et al. Experimental and numerical investigation of the size effect of rockfill particles on crushing strength[J]. *Granular Matter*, 2023,25(4).
6. YIN Fu-shun, LI Sa, LIU Xin. Experimental study on single particle strength and compression properties of calcareous coarse sand[J]. *Rock and Soil Mechanics*, 2023, 44(4): 1120-1129, 1152.
7. XUEHUI W, YUANQIANG C, SIFA X, et al. Effects of size and shape on the crushing strength of coral sand particles under diametral compression test[J]. *Bulletin of Engineering Geology and the Environment*, 2020(prepublish): 1-11.
8. HUANG J, XU S, YI H, et al. Size effect on the compression breakage strengths of glass particles[J]. *Powder Technology*, 2014,268: 86-94.
9. WANG Lei, JIANG Xiang, XIAO Yang, et al. Experimental research on size effect and avalanche dynamics characteristics of calcareous sand particles[J]. *Chinese Journal of Geotechnical Engineering*, 2021, 43(6): 1029-1038.
10. MA P, CHEN Y. A skeleton weakening constitutive model for breakable particle soils[J]. *Computers and Geotechnics*, 2025,179: 106968.
11. WANG W, COOP M R. An investigation of breakage behaviour of single sand particles using a high-speed microscope camera[J]. *Géotechnique*, 2016,66(12): 984-998.
12. MENG Min-qiang, YUAN Zheng-xin, JIANG Xiang. Experimental study of the single-particle crushing-strength-size effect of calcareous sand-quartz sand[J]. *Scientia Sinica: Technologica*, 2022, 52(7): 1035-1047.
13. MENG M, SUN Z, WANG C, et al. Size Effect on Mudstone Strength During Freezing-Thawing Cycle[J]. *Environmental Geotechnics*, 2019: 1-13.
14. WANG Y, SHAO C, XU Y. Fractal crushing of solid particles[J]. *KSCE Journal of Civil Engineering*, 2017, 21: 987-993.
15. Weibull W. A statistical distribution function of wide applicability. *J Appl Mech*, 1951, 13: 293-297
16. ZHANG Y D, BUSCARNERA G, EINA V I. Grain size dependence of yielding in granular soils interpreted using fracture mechanics, breakage mechanics and weibull statistics[J]. *Géotechnique*, 2016, 66: 149-160.

**Open Access** This chapter is licensed under the terms of the Creative Commons Attribution-NonCommercial 4.0 International License (<http://creativecommons.org/licenses/by-nc/4.0/>), which permits any noncommercial use, sharing, adaptation, distribution and reproduction in any medium or format, as long as you give appropriate credit to the original author(s) and the source, provide a link to the Creative Commons license and indicate if changes were made.

The images or other third party material in this chapter are included in the chapter's Creative Commons license, unless indicated otherwise in a credit line to the material. If material is not included in the chapter's Creative Commons license and your intended use is not permitted by statutory regulation or exceeds the permitted use, you will need to obtain permission directly from the copyright holder.

